S-nitrosylation of AMPA receptor GluA1 regulates phosphorylation, single-channel conductance, and endocytosis

Balakrishnan Selvakumar[a], Meagan A. Jenkins[b], Natasha K. Hussain[a], Richard L. Huganir[a,c], Stephen F. Traynelis[b], and Solomon H. Snyder[a,d,e,1]

[a]Solomon H. Snyder Department of Neuroscience and Departments of [d]Psychiatry and Behavioral Sciences, [e]Pharmacology and Molecular Sciences, and [c]Howard Hughes Medical Institute, The Johns Hopkins University School of Medicine, Baltimore, MD 21205; and [b]Department of Pharmacology, Emory University School of Medicine, Atlanta, GA 30322

Contributed by Solomon H. Snyder, December 6, 2012 (sent for review November 13, 2012)

NMDA receptor activation can elicit synaptic plasticity by augmenting conductance of the AMPA receptor GluA1 subsequent to phosphorylation at S831 by Ca^{2+}-dependent kinases. NMDA receptor activation also regulates synaptic plasticity by causing endocytosis of AMPA receptor GluA1. We demonstrate a unique signaling cascade for these processes mediated by NMDA receptor-dependent NO formation and GluA1 S-nitrosylation. Thus, S-nitrosylation of GluA1 at C875 enhances S831 phosphorylation, facilitates the associated AMPA receptor conductance increase, and results in endocytosis by increasing receptor binding to the AP2 protein of the endocytotic machinery.

AMPA receptors (AMPARs) are tetramers in their physiologic form, with GluA1 being one of the more important regulatory subunits (1). Synaptic plasticity frequently is mediated by activation of NMDA receptors (NMDARs), which can modulate surface expression and single-channel conductance of AMPARs during the early phase of long-term potentiation (LTP) (1, 2). Phosphorylation of S831 of GluA1 mediates such plasticity, as phosphorylation of this site increases during LTP (3, 4), and mutant mice overexpressing a phosphomimetic S831D mutation display enhanced AMPAR conductance and LTP (5, 6).

Mechanisms whereby NMDAR transmission augments AMPAR conductance have been unclear. NMDAR activation leads to calcium entry, which stimulates catalytic activity of neuronal nitric oxide synthase (nNOS) (7, 8). NO (nitric oxide) signals by activating guanylate cyclase, and by S-nitrosylating cysteines of many target proteins (9, 10). NO regulates AMPARs by targeting AMPAR-interacting proteins that determine receptor surface expression. Thus, physiologic S-nitrosylation of NSF (*N*-ethylmaleimide sensitive factor) elicits enhanced surface expression of GluA2 (11). Transmembrane AMPAR regulatory proteins are prominent auxiliary proteins for AMPARs, with stargazin being the best characterized (12). NMDAR transmission triggers S-nitrosylation of stargazin, which increases surface expression of GluA1 (13).

The surface expression of AMPARs that determines synaptic plasticity is regulated by endocytosis because inhibitors of endocytosis block AMPAR removal from the plasma membrane, resulting in increased surface expression of AMPARs and long term depression (LTD) (14). Although NO has been implicated in regulation of protein endocytosis (15), its role in regulating AMPAR endocytosis is unknown.

In the present study, we show that GluA1 is physiologically S-nitrosylated under basal conditions, with increased nitrosylation upon NMDAR stimulation. Moreover, the NMDAR-dependent phosphorylation of GluA1-S831 is regulated by endogenous NO, which acts by S-nitrosylating GluA1-C875. These events regulate single-channel conductance of GluA1, as the increase of such conductance by phosphorylation is markedly slowed in GluA1-C875S mutants. Endocytosis of AMPAR also is regulated by nitrosylation of GluA1-C875, because the C875S mutant of GluA1 reduces AMPAR endocytosis in neuronal cells and decreases binding to AP2 protein of the endocytotic machinery. Thus, a signaling pathway exists whereby NMDA transmission triggers S-nitrosylation of GluA1 to facilitate receptor phosphorylation and the phosphorylation-dependent increase in single-channel conductance. In addition, under conditions that induce endocytosis of the receptor, nitrosylation of GluA1 facilitates endocytosis via increased binding to AP2.

Results

In HEK293 cells overexpressing GluA1, the NO donor cysteine-NO elicits robust S-nitrosylation of GluA1 receptors (Fig. 1*C*), suggesting that GluA1 can be nitrosylated. The intracellular, cytosolic portion of GluA1, which is the locus of multiple post-translational modifications (1), contains three cysteines: C811, C825, and C875 (Fig. 1*D*). Mutations of each of these cysteines reduces GluA1 S-nitrosylation in HEK293 cells constitutively overexpressing nNOS (Fig. 1 *A* and *B*), suggesting that all three potentially may be S-nitrosylated under endogenous conditions of NO generation. Nitrosylation of GluA1 seen in heterologous systems overexpressing both GluA1 and nNOS (Fig. 1 *A* and *B*) might be higher than when the proteins are expressed under physiologic conditions. Endogenous GluA1 is physiologically S-nitrosylated in intact brain, in both an nNOS-dependent and ascorbate-dependent manner (Fig. 1 *E* and *F*).

GluA1-S831 is phosphorylated by protein kinase C (PKC) and calmodulin-dependent protein kinase II (CaMKII) in vitro and in vivo (3, 16, 17). We show that this phosphorylation is influenced by NO. Thus, phosphorylation of GluA1-S831 elicited by phorbol ester stimulation of PKC is markedly enhanced in HEK293 cells expressing nNOS (Fig. 2 *C–E*). In basal HEK293 cells, the NO donor cysteine-NO enhances GluA1-S831 phosphorylation (Fig. 2 *A* and *B*), suggesting that NO in and of itself can increase phosphorylation of GluA1-S831 under basal conditions. GluA1-S831 phosphorylation is greatly reduced by mutating C875 and, to a lesser degree, C811 and C825 (Fig. 2 *D* and *E*). These data suggest that the main site of S-nitrosylation within the GluA1 C-terminal domain that regulates GluA1-S831 phosphorylation occurs at C875. Phosphorylation of GluA1-S831 by the phorbol ester PMA (phorbol myristyl acetate) increases at 5 and 10 min, time points at which the GluA1-C875S mutant has less phosphorylation (Fig. 2 *F* and *G*).

Stimulation of GluA1-S831 phosphorylation requires endogenous NO. In neocortical neuronal cultures treated with NMDA, phosphorylation of GluA1 at S831 is reduced in nNOS knockout cultures (Fig. 3 *A* and *B*). NMDA treatment of neuronal cells in culture activates both synaptic and extrasynaptic NMDARs. However, treatment with glycine, which is a coagonist with glutamate at NMDARs, in conjunction with the GABA antagonist bicuculline, results in higher ambient levels of glutamate in the synaptic cleft (18). The phosphorylation of GluA1-S831 under

Author contributions: B.S., R.L.H., and S.H.S. designed research; B.S., M.A.J., and N.K.H. performed research; B.S., M.A.J., N.K.H., R.L.H., S.F.T., and S.H.S. analyzed data; and B.S., M.A.J., R.L.H., S.F.T., and S.H.S. wrote the paper.

The authors declare no conflict of interest.

[1]To whom correspondence should be addressed. E-mail: ssnyder@jhmi.edu.

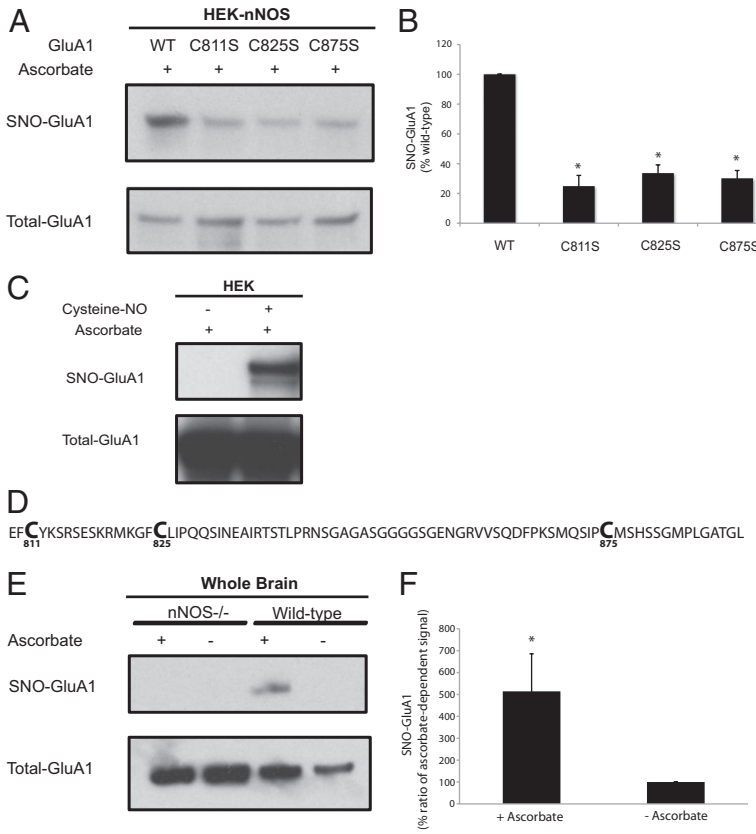

Fig. 1. Endogenous S-nitrosylation of GluA1. (*A*) HEK-nNOS cells stably expressing nNOS were transfected with WT GluA1 or cysteine mutants of GluA1, and lysates were analyzed by the biotin-switch assay. (*B*) Quantification of experiments in *A*. (*C*) HEK cells transfected with GluA1 were treated with 100 μM of cysteine-NO for 10 min, and lysates later were analyzed by the biotin-switch assay, which demonstrates the presence of S-nitrosylated cysteines. (*D*) Amino acid sequence of the cytosolic C-terminal tail of GluA1. (*E*) Brain lysates obtained from WT or nNOS knockout ($nNOS^{-/-}$) animals were analyzed by the biotin-switch assay to determine physiologic nitrosylation of GluA1. The ascorbate dependence demonstrates specifically the presence of S-nitrosylation. (*F*) Quantification of ascorbate-dependent signal for nitrosylated-GluA1 in WT animals. Data are means ± SEM, $P < 0.05$. All Western blots show representative images of experiments performed at least three times.

the glycine/bicuculline treatment regimen is virtually abolished in nNOS knockout cultures (Fig. 3 *C* and *D*). Furthermore, the glycine/bicuculline treatment increases nitrosylation of GluA1 (Fig. 3*E*). Although the effect of nNOS and NO on GluA1-S831 phosphorylation might be the result of effects on PKC or CaMKII, this possibility is unlikely because S-nitrosylation of these two enzymes reduces their activity (19–21). Also, a role for guanylate cyclase in mediating the activating effects of NO on GluA1-S831 phosphorylation is unlikely because inhibition of cyclic guanylate kinase increases glycine-stimulated phosphorylation of GluA1-S831 (22). Thus, GluA1 phosphorylation at S831 is enhanced by the physiologic generation of NO and subsequent S-nitrosylation of GluA1 at C875.

Phosphorylation of GluA1 at S831 increases apparent single-channel conductance of GluA1 by enhancing the proportion of openings to higher conductance levels (1, 5). We included purified, activated CaMKII in the intracellular recording solution to phosphorylate GluA1-S831. We chose to use CaMKII in these experiments for two reasons. First, CaMKII phosphorylation of GluA1 Ser831 and the functional effects thereof are well documented by many laboratories, whereas PKC phosphorylation of this residue is less studied (3, 5, 17, 18, 23). There is a clear, robust, and reproducible effect of purified CaMKII on GluA1 Ser831 that we used in our laboratory previously and that we sought to take advantage of in patch-clamp experiments here. Furthermore, CaMKII has a clear role in LTP and is activated by NMDAR stimulation. Because we believe the relationship between C875S nitrosylation and Ser831 phosphorylation is important for synaptic plasticity and links NMDAR activation to AMPAR modulation, we chose to use CaMKII in these functional experiments.

HEK-nNOS cells expressing stargazin, protein kinase inhibitor (to inhibit endogenous PKA activity), and GluA1 wild-type (WT) and C875S mutant receptors were used in patch-clamp experiments. GluA1 also contained the L497Y mutation to inhibit receptor desensitization. Preventing desensitization allows slow washout of a maximally effective concentration of glutamate (1 mM) to produce a slowly changing current to which variance analysis may be applied (Fig. 4*A*). Nonlinear least-squares fitting of these data to Eq. **1** (*Materials and Methods*) was used to determine the weighted mean conductance (γ_{MEAN}) for the recombinant GluA1 receptors (Fig. 4*B*). Conductance measurements were collected every 2 min after outside-out patch excision for both GluA1 WT and GluA1-C875S receptors in the presence and absence of CaMKII (Fig. 4*C*). Conductance of WT GluA1 is enhanced by CaMKII within 2 min of pulling the patch and remains high throughout the recording period. By contrast, the conductance of GluA1-C875S receptors increases slowly over the course of the recording (Fig. 4*C*). Thus, the impact of the C875S mutation on GluA1 conductance is most apparent at early times. For example, 2 min after excising the membrane patch to allow purified CaMKII to access the intracellular surface of the membrane, the CaMKII-mediated conductance increase in WT GluA1 is maximal (160% of control). By contrast, no significant increase in conductance for the GluA1-C875S mutant is observed at 2 min (Fig. 4*C*). It is not until 8 min after breaking through the membrane and excising the patch that CaMKII treatment increases channel conductance of the GluA1-C875S mutant to the same extent as WT channels (Fig. 4*C*). In addition, the basal conductance of GluA1-C875S receptors, in the absence of CaMKII, at $t = 0$ is significantly lower than the basal conductance of WT GluA1 receptors (Fig. 4*C*). Conductance measurements at each time point were normalized and plotted against time to illustrate the rate at which CaMKII enhances conductance of GluA1 and GluA1-C875S receptors. These data were fit to an exponential function of the form $y = 1 - e^{(-time/\tau)}$ to measure the time constant τ of the CaMKII-mediated conductance increase. The time constant describing the conductance increase in WT channels of about 1 s is increased approximately sevenfold for the mutant channels (Fig. 4*D*).

Endocytosis of AMPAR is regulated by nitrosylation of GluA1-C875. WT GluA1 receptors tagged with GFP expressed in neuronal cells undergo robust endocytosis upon stimulation

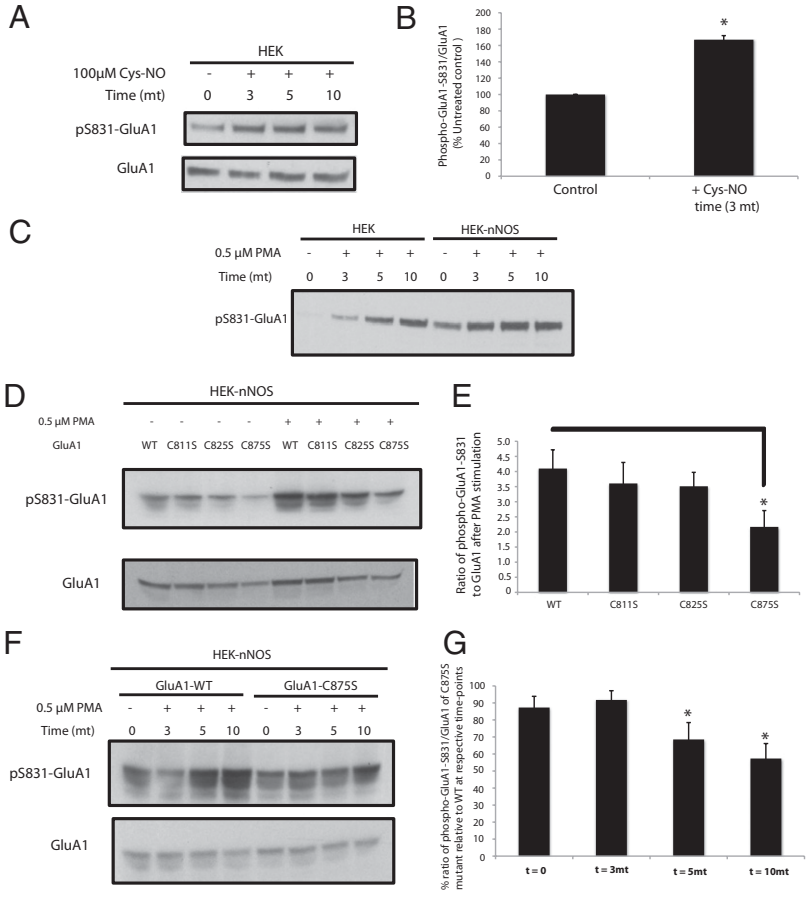

Fig. 2. Endogenous phosphorylation of S831-GluA1 requires nitric oxide. (*A*) HEK cells expressing GluA1 were treated with 100 μM cysteine-NO for various time points, and lysates were analyzed by Western blot for phospho-S831-GluA1. (*B*) Quantification of experiment in *A*; data are mean ± SEM (*$P < 0.05$, Student *t* test). (*C*) HEK cells and HEK-nNOS cells stably expressing nNOS were transfected with GluA1 and stimulated with 0.5 μM PMA for various time points, and lysates were analyzed by Western blot for phospho-S831 GluA1. (*D*) HEK-nNOS cells expressing WT GluA1 or cysteine mutants of GluA1 were treated with 0.5 μM PMA for 10 min, and lysates were analyzed by Western blot for phospho-S831-GluA1. (*E*) Quantification of experiments in *D*; data are mean ± SEM (*$P < 0.05$, Student *t* test). (*F*) HEK-nNOS cells expressing WT or C875S-GluA1 were treated with 0.5 μM PMA for various time points, and lysates were analyzed by Western blot for phospho-S831-GluA1. All Western blots show representative images of experiments performed at least three times. (*G*) Quantification of experiment in *F*; data are mean ± SEM (*$P < 0.05$, Student *t* test).

with 40 μM NMDA for 5 min (Fig. 5 *A* and *B*). However, the NMDA-stimulated endocytosis is significantly reduced with the GluA1-C875S mutant (Fig. 5 *A* and *B*). To test the mechanism of action of NO in regulating endocytosis of GluA1, we performed binding studies using HEK-nNOS cells overexpressing GluA1 and endogenous AP2 protein of the endocytotic machinery. The binding between WT GluA1 and AP2 is increased by treatment with 100 μM AMPA for 10 min. Pretreatment with nNOS inhibitor reduces both basal and AMPA-stimulated binding between GluA1 and AP2. Similarly, expression of GluA1-C875S mutant reduces AMPA-stimulated binding of the mutant receptor to AP2. Furthermore, in neuronal cells, pretreatment with the nNOS inhibitor VNIO significantly reduces the AMPA-induced increase in binding between GluA1 and AP2 (Fig. 5).

Discussion

In the present study, we demonstrate a signaling cascade that modulates both the augmentation of AMPAR conductance secondary to GluA1-S831 phosphorylation and endocytosis of the receptor. This signaling pathway may be important during synaptic plasticity. NMDAR neurotransmission increases intracellular calcium levels that stimulate nNOS to generate NO. The newly formed NO S-nitrosylates GluA1 at C875. This event facilitates phosphorylation of the receptor at S831, which in turn accelerates the increase in AMPAR conductance. Furthermore, the basal conductance of GluA1-C875S receptors also is significantly less than that of WT GluA1 receptors. Finally, neurotransmission regulates endocytosis of GluA1, which is regulated by increased binding of nitrosylated GluA1-C875 to AP2. Thus, the C875S mutation of GluA1 substantially slows the phosphorylation of S831, which consequently slows the CaMKII-associated increase in single-channel conductance, whereas it decreases the binding to AP2 and thereby reduces receptor endocytosis.

Increased conductance and surface expression of AMPARs in the synapse underlie LTP, the best-studied form of memory storage and learning at excitatory synapses. Posttranslational regulation of AMPARs through protein–protein interaction, phosphorylation, and palmitoylation has been widely described as an important mode of regulating AMPAR function [reviewed in Shepherd and Huganir (1)]. Although NO previously was implicated in diverse forms of synaptic plasticity, including LTP (8), mechanisms accounting for these effects have been obscure. Some of the currently proposed mechanisms ascribing a role for NO in synaptic plasticity involve regulation of AMPAR surface expression by NO. For instance, S-nitrosylation of NSF enhances binding to GluA2, thereby increasing surface expression of GluA2 (11). Inhibition of the NO/cGMP cascade reduces GluA1 surface expression (22). Stargazin, an AMPAR auxiliary protein that binds to a large fraction of different types of AMPAR subunits (24) and facilitates the phosphorylation-mediated increase in heteromeric GluA1/GluA2 receptor conductance (5), also enhances GluA1 surface expression when nitrosylated (13). Postsynaptic density protein-95 (PSD-95), a scaffolding protein that regulates AMPAR clustering in the postsynaptic density, is reciprocally regulated by S-nitrosylation and palmitoylation (25). However, none of these studies implicates NO in directly regulating AMPAR phosphorylation and single-channel conductance, or endocytosis. It is widely believed that NMDAR-stimulated calcium entry, activation of CaMKII, and subsequent phosphorylation of GluA1-S831 to increase channel conductance are important signals underlying early-phase LTP (1, 2, 5). Rapid endocytosis of AMPARs regulates their synaptic surface expression and therefore is critical in modulation of LTD, a form of synaptic plasticity (14). The NMDAR-stimulated calcium influx critical for LTP (2), and involved in AMPAR endocytosis (26), also triggers S-nitrosylation of proteins as the result of

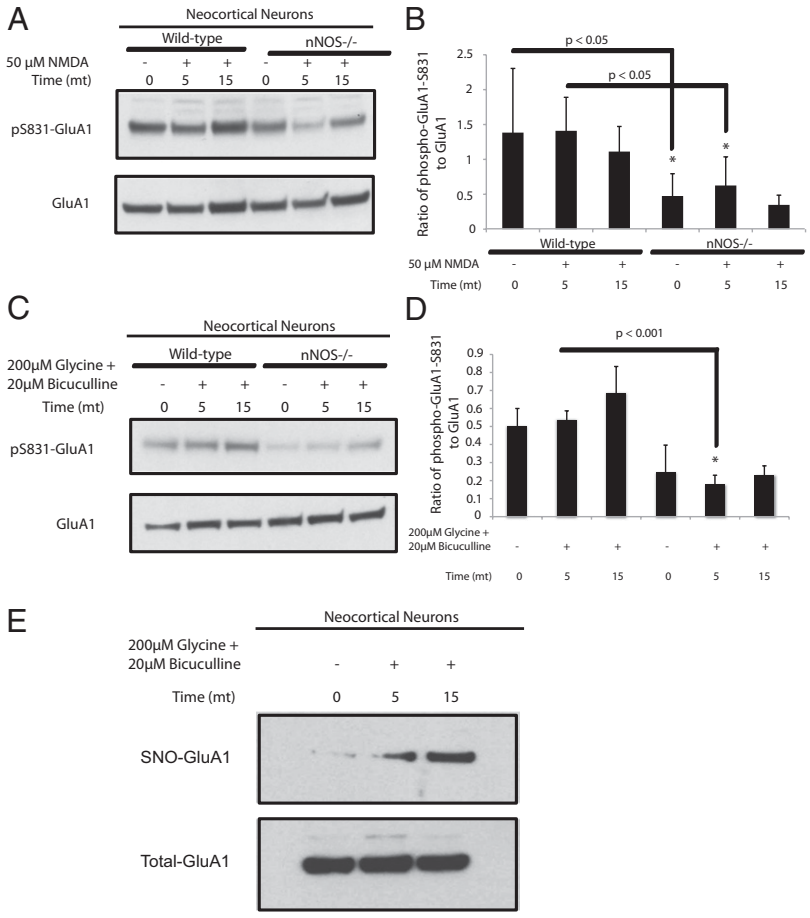

Fig. 3. In dissociated cultures of neocortical neurons, stimulation of NMDAR increases nitrosylation of GluA1, and the receptor-stimulated increase in phospho-S831-GluA1 is dependent on NO. (*A*, *C*, and *E*) Dissociated cultures of neocortical neurons obtained from WT or nNOS$^{-/-}$ animals in *A* were pretreated with 1 μM TTX and 20 μM CNQX for 30 min followed by 50 μM NMDA for 5 and 15 min, or in *C* and *E* were pretreated with 0.5 μM TTX and 1 μM strychnine for 30 min followed by 200 μM glycine and 20 μM bicuculline for 5 and 15 min. Lysates were analyzed by Western blot for phospho-S831-GluA1 and phospho-S845-GluA1 in *A* and phospho-S831-GluA1 alone in *C*, and by the biotin-switch assay for nitrosylated GluA1 in *E*. (*B* and *D*) Quantification of phospho-S831-GluA1 from experiments in *A* and *C*, respectively. Quantification of data is means ± SEM, $P < 0.05$. All Western blots show representative images of experiments performed at least three times.

activation of nNOS (7, 11, 13). Our findings establish that AMPAR phosphorylation, conductance, and endocytosis are physiologically regulated by GluA1 S-nitrosylation at C875, and may be a mechanism by which NO regulates synaptic plasticity.

The regulation of a prominent site of GluA1 phosphorylation by S-nitrosylation advances our fundamental understanding of the molecular features of GluA1 regulation, specifically the role of NO in regulating AMPAR function. Moreover, S-nitrosylation increasingly is appreciated as an important posttranslational modification of proteins. Regulation of a site of phosphorylation by nitrosylation of the same protein as observed for GluA1 in this study, and as shown earlier for eNOS (27), might reflect a general mechanism that influences many diverse biological processes.

The current data, in conjunction with past data from our laboratory, reveal a complex picture wherein NO regulates AMPAR function by targeting stargazin, PSD-95, and GluA1. Under basal and mild conditions of NMDAR stimulation, NO facilitates stargazin-mediated effects on surface expression of AMPARs in cerebellar granule as well as neocortical neurons, whereas it promotes receptor phosphorylation of the site that increases conductance in neocortical neurons. These effects, along with the effect of NO in increasing phosphorylation-mediated single-channel conductance of GluA1 in heterologous cells, suggest a role for NO in LTP. NO decreases palmitoylation of PSD-95 in hippocampal and cerebellar granule neurons, and decreases synaptic clustering of PSD-95 in cerebellar granule neurons under conditions of basal and robust stimulation of NMDARs. These effects might influence clustering of AMPARs under similar conditions. Also, NO promotes internalization of AMPARs under conditions that result in NMDAR-dependent endocytosis in hippocampal neurons, suggesting a role for NO in LTD.

Materials and Methods

Cell Culture. Experiments involving animals were approved by the Johns Hopkins University Animal Care and Use Committee (ACUC). HEK293 and HEK-nNOS cells were cultured in DMEM with FBS (10% vol/vol), penicillin (200 U/mL), streptomycin (200 μg/mL), L-glutamine (2 mM), and tylosin (8 μg/mL) (Sigma-Aldrich). Dissociated neocortical neurons were prepared from embryonic day 18–19 mouse brains in neurobasal media with B27 supplement (Gibco, BRL). The neuronal cells were used for experiments between 7–14 d in vitro.

Plasmids and Transfections. The flip splice variant of the rat GluA1 cDNA was subcloned into the pRK5 vector and was used in all biochemical experiments. The single cysteine mutations of GluA1 (C811S, C825S, and C875S) were made using standard protocols for Pfu Turbo DNA polymerase (Stratagene). GluA1 plasmids were transfected into HEK cells by using Polyfect (Qiagen) following manufacturer's instructions. For all biochemical experiments, transfected cells were lysed within 24 h.

Antibodies and Reagents. Mouse monoclonal and rabbit polyclonal anti-GluA1 antibody was prepared in the Huganir Laboratory. Rabbit anti-pS831-GluA1 was prepared in the Huganir Laboratory and also obtained from Millipore/Chemicon. Rabbit anti-pS845-GluA1 was prepared in the Huganir Laboratory. Mouse monoclonal anti-AP2 antibody was obtained from BD Transduction Laboratories. TTX, 6-cyano-7-nitroquinoxaline-2,3-dione (CNQX), bicuculline, and NMDA used in biochemical experiments were purchased from Tocris Bioscience. Cysteine-NO was prepared by treating equimolar amounts of sodium nitrite and L-cysteine hydrochloride. All other biochemical reagents were purchased as indicated or from Sigma-Aldrich.

Western Blot Analysis. Both neuronal cells and HEK cells were lysed in buffer containing 1% Triton X-100 along with proteinase and phosphatase inhibitors. Lysates were extracted for 1 h at 4 °C followed by centrifugation at 16,000 × *g* in a microfuge. Protein was assayed from the resultant supernatant, and equal amounts of protein were mixed with Laemelli buffer and resolved using standard electrophoresis and Western blot methods.

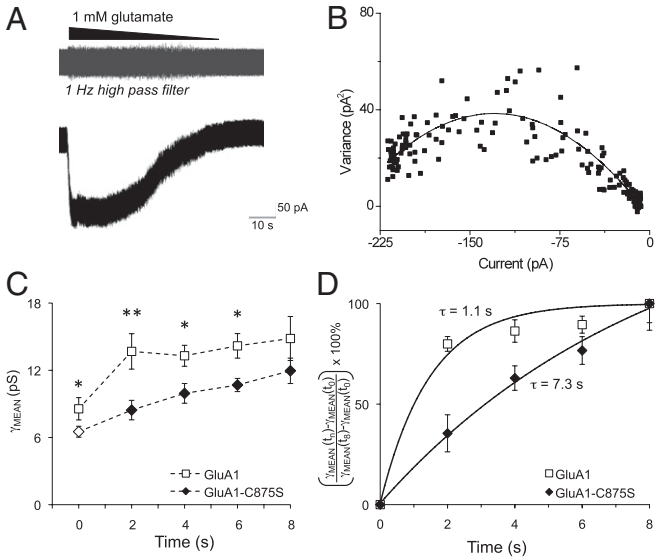

Fig. 4. The GluA1-C875S mutation slows the effect of CaMKII on AMPAR conductance. (*A*) Representative GluA1 receptor current trace from an outside-out membrane patch excised from a transiently transfected HEK cell. Non-desensitizing receptors allow for the slow wash of a maximally effective concentration of glutamate (1 mM) to produce a slowly changing current to which variance analysis can be applied. The gray trace above shows the recording after a 1-Hz high-pass filter, highlighting the relationship between channel-mediated noise and current amplitude during glutamate washout. (*B*) A representative current–variance relationship is shown for the patch in *A*. Nonlinear least-squares fitting of these data to Eq. **1** (*Materials and Methods*) was used to determine γ_{MEAN} for GluA1. (*C*) Conductance measurements were collected every 2 min after outside-out patch excision for both GluA1 WT receptors (□) and GluA1-C875S receptors (♦) in the presence of CaMKII. Both receptors also contain the nondesensitizing L497Y mutation. Open symbols at t = 0 indicate the basal conductance value of WT and mutant GluA1 receptors in the absence of CaMKII. $^{**}P < 0.001$ $^{*}P < 0.05$ by two-way ANOVA with Tukey's test. Conductance at t = 8 min was not significantly different between WT and GluA1-C875S receptors. (*D*) Conductance measurements at each time point were normalized as indicated on the *y*-axis and plotted against time to illustrate the rate at which CaMKII enhances conductance of GluA1 (□) and GluA1-C875S receptors (♦). The time constant, τ, of the CaMKII-mediated conductance increase was measured by fitting these data to an exponential function of the form $y = 1 - e^{(-time/\tau)}$.

Biotin Switch Assay. Whole-brain extracts were prepared by homogenizing snap-frozen brain tissue in lysis buffer (250 mM Hepes/1 mM EDTA/0.1 mM neocuproine, pH 7.7, with 1% Triton X-100, 200 μM deferoxamine, and proteinase inhibitors) using a Teflon-on-glass homogenizer, followed by passage through a 26-gauge needle and syringe ~10 times. Lysates were extracted for about 15–30 min at 4 °C, followed by centrifugation at 14,000 rpm in a microfuge. Cell extracts from cultured cells were prepared similarly but without using the homogenizer. Cell extracts were analyzed by the biotin-switch assay as described before with modifications (10). This assay is based on the selective reduction of nitrosylated cysteines of proteins using ascorbate, followed by capping of the reduced cysteine with a sulfhydryl reactive group that also contains a biotin tag. The biotinylated proteins then are enriched by affinity purification using streptavidin beads. In brief, extracts were treated with methyl methanethiosulfonate (0.1%) and SDS (2.5%) at 50 °C for 20 min with constant agitation. Proteins were precipitated with acetone, and the precipitate was labeled with biotin-HPDP (N-[6-(Biotinamido)hexyl]-3′-(2′pyridyldithio)propionamide) (0.5 mM) (Soltec Ventures) with or without ascorbate (50 mM) for 90 min at room temperature. Proteins were reprecipitated with acetone, and the precipitate was either incubated with anti-GluA1 antibody for immunoprecipitation, followed by elution with the GluA1 epitope, or added directly to streptavidin beads (Pierce). The eluate from the immunoprecipitation was treated similarly with the streptavidin beads. The eluate from the streptavidin beads was separated by SDS/PAGE and analyzed by Western blotting.

Neuronal Culture and Immunostaining. Hippocampal neurons were dissected from embryonic day 19 (E19) Sprague–Dawley rat embryos, plated onto coated glass coverslips (30 μg/mL poly D-lysine and 2.5 μg/mL laminin), and cultured in Neurobasal Medium (Invitrogen) with B27 (Invitrogen), 0.5 mM glutamine, and 12.5 μM glutamate. Neurons were transfected after 18–19 d in vitro using Lipofectamine 2000 (Invitrogen) according to the manufacturer's instructions. Forty-eight hours after transfection, neurons were left untreated or received 40 μM NMDA for 3 min in conditioned media before processing for immunostaining. Surface-expressing GFP-GluA1 WT or GFP-GluA1 C875S was labeled by incubating live neurons in artificial cerebrospinal fluid for 15 min at 4 °C with rabbit anti-GFP antibodies (JH4030 antibody, raised against a GFP fusion protein). Neurons then were washed twice with ice-cold PBS and fixed with 4% paraformaldehyde and 4% sucrose in PBS (room temperature, 10 min). Total AMPAR overexpression was visualized by subsequent overnight labeling at 4 °C with chicken anti-GFP antibodies (Abcam) in 1× GDB buffer (30 mM phosphate buffer, pH 7.4, containing 0.2% gelatin, 0.5% Triton X-100, and 0.8 M NaCl) at 4 °C, followed by secondary antibodies for 2–4 h in 1× GDB buffer at room temperature.

Microscopy and Quantification. Fixed neurons were imaged with an LSM510 confocal microscope system (Zeiss). Confocal z-series image stacks encompassing entire dendrite segments were compressed into a single plane and analyzed using MetaMorph software (Universal Imaging). For integrated intensity quantification (i.e., average cluster intensity per unit area), different immunostained channels were parsed into separate images. Five dendritic segments of 50 μm collected from at least 20 neurons per condition were outlined, and a threshold level for each channel was set manually to exclude diffuse background staining, leaving only the puncta visible; the same threshold level was used for each neuron within an experiment. Statistical significance between samples was calculated using ANOVA.

Maintenance and Transfection of HEK Cells Used in Electrophysiology. All cell biology reagents were obtained from Gibco (Invitrogen). DMEM with GlutaMAX supplemented with 10% (vol/vol) FCS, 100 U/mL of penicillin, 100 μg/mL of streptomycin, and 8 μg/mL of tylosin was used to maintain HEK-nNOS cells. Cells were grown at 5% CO_2, 95% O_2 at 37 °C either on 60-mm polystyrene culture dishes or poly-D-lysine–coated (Millipore) 8-mm glass coverslips contained in 24-well tissue culture plates. Trypsin-EDTA (0.05%) was used to passage cells. FuGENE6 was used for transfection of all cDNAs according to the manufacturer's protocol. At time of transfection, DMEM was supplemented with 200 μM NBQX (2,3-dihydroxy-6-nitro-7-sulfamoyl-benzo[f]quinoxaline-2,3-dione, a competitive AMPAR antagonist; Tocris) to protect against excitotoxicity.

Recording and Analysis of Macroscopic Currents from Excised Membrane Patches. Outside-out membrane patches were excised from transiently transfected HEK-nNOS cells using thin-walled borosilicate micropipettes (World Precision Instruments). Pipettes had a tip resistance of 4–6 MOhm. Internal solutions were composed of (in millimolars) 110 gluconic acid, 110 CsOH, 30 CsCl, 4 NaCl, 5 Hepes, 4.37 EGTA, 2.1 $CaCl_2$, 2.27 $MgCl_2$, 0.1 spermine (Sigma-Aldrich), 4 ATP, and 0.3 GTP. The pH was adjusted to 7.3 with CsOH. For some experiments, internal solution was supplemented with 25,000 U/mL purified CaMKII, activated according to the manufacturer's protocol (New England Biolabs). External recording solution for all experiments was composed of (in millmolars) 150 NaCl, 10 Hepes, 3 KCl, 1 $CaCl_2$, 1 $MgCl_2$, pH 7.4; 310–330 mOsm. Currents were recorded at room temperature (23 °C) at a holding potential (V_{HOLD}) of –60 mV. Data were recorded on a HEKA EPC9 amplifier, and the current response was filtered at 5 kHz (–3 dB) and digitized at a sampling rate of 20 kHz. ChanneLab (Decatur, GA) (Synaptosoft Inc.) was used to perform stationary variance analysis of macroscopic currents, as previously described (28, 29). Briefly, variance (σ^2) may be related to the macroscopic (*I*) and unitary current (*i*) amplitude by

$$\sigma^2 = i\,I - (I^2/N), \qquad [1]$$

where *N* is the number of channels. Nonlinear least-squares fitting of this equation to the data was used to determine the unitary current and number of channels. The unitary current is a weighted mean average of all single-channel conductance levels (29). Chord conductance (γ_{NOISE}) was determined assuming a 0-mV reversal potential.

Statistical Methods Used in Electrophysiology. Results are expressed as mean ± SEM. Statistical analysis of time dependence was performed with a two-way ANOVA with multiple comparisons, where t = 0 represents a conductance measurement as quickly as could be measured after excising a patch. Tukey's post hoc test was used to determine time points at which conductance was significantly different in WT versus mutant GluA1 receptor. $P < 0.05$ was considered statistically significant. Power of all statistical tests was at least 0.8.

Statistical Methods Used in Biochemistry. Results are expressed as mean ± SEM. Statistical analysis $^{*}P$ value of less than 0.05 was considered statistically significant.

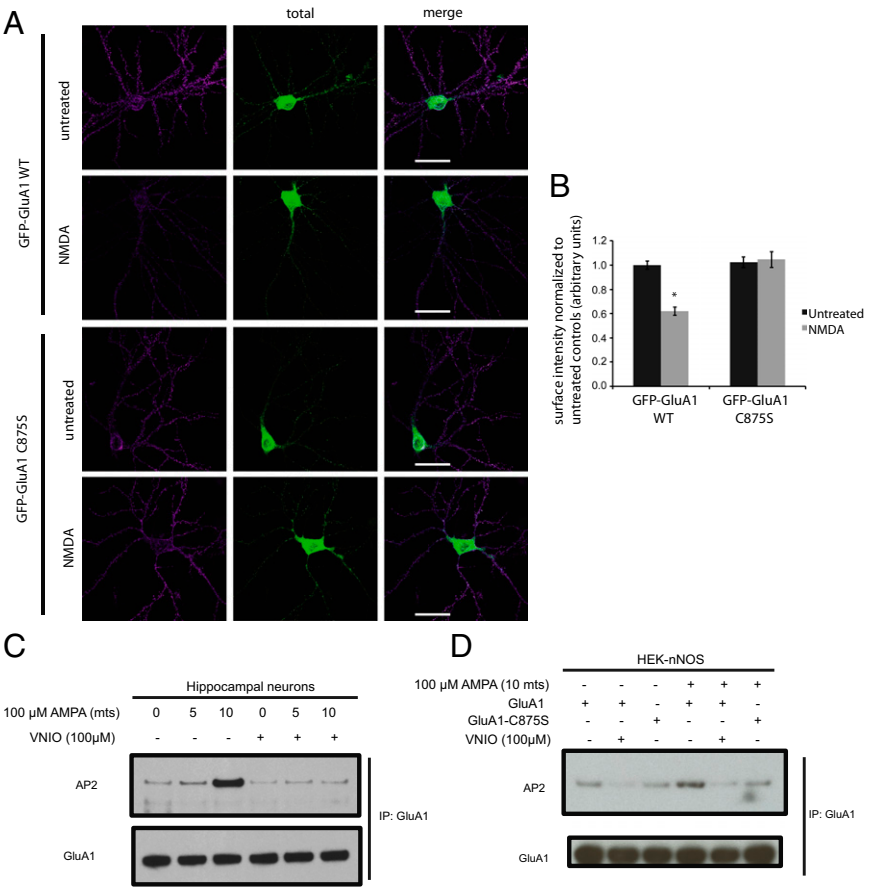

Fig. 5. GluA1-C875S mutation abrogates endocytosis and binding to AP2. (*A*) Representative images of hippocampal neurons transfected with WT or C875S mutant GFP-GluA1, with or without 3-min treatment of 40 μM NMDA, and immunostained for surface and total GFP expression. Scale bars, 40 μm. (*B*) Quantification of mean integrated surface GFP-GluA1 cluster intensity in dendritic segments normalized to untreated total GFP-GluA1 WT expression. Error bars indicate mean ± SEM, $*P < 0.0001$ relative to untreated WT control, ANOVA, and Fisher's Partial Least Squares Difference; $n \geq 21$ neurons for each condition. (*C*) Representative immunoblot of AP2 after immunoprecipitation with GluA1 antibody from hippocampal neuronal cells that were stimulated with 100 μM AMPA for 5 and 10 min with or without pretreatment with the nNOS inhibitor VNIO. (*D*) Representative immunoblots of AP2 after immunoprecipitation with GluA1 antibody from HEK-nNOS cells expressing either GluA1 WT or GluA1-C875S mutant. Cells were stimulated with 100 μM AMPA with or without pretreatment with the nNOS ihibitor VNIO.

ACKNOWLEDGMENTS. We thank Roxanne Barrow for excellent technical help; Lynda Hester for preparing dissociated neuronal cultures of the neocortex; Masoumeh Saleh for maintenance and genotyping of nNOS knockout mice; Gareth Thomas, Jean-Claude Béïque, and Myoung-Goo Kang for discussions pertaining to AMPAR biology; and past and present members of the Snyder laboratory for helpful discussions. This work was supported by US Public Health Service Grants MH18501 (to S.H.S.), NS36715 (to R.L.H.), and NS068464 (to S.F.T.).

1. Shepherd JD, Huganir RL (2007) The cell biology of synaptic plasticity: AMPA receptor trafficking. *Annu Rev Cell Dev Biol* 23:613–643.
2. Lisman J, Yasuda R, Raghavachari S (2012) Mechanisms of CaMKII action in long-term potentiation. *Nat Rev Neurosci* 13(3):169–182.
3. Barria A, Muller D, Derkach V, Griffith LC, Soderling TR (1997) Regulatory phosphorylation of AMPA-type glutamate receptors by CaM-KII during long-term potentiation. *Science* 276(5321):2042–2045.
4. Lee HK, Barbarosie M, Kameyama K, Bear MF, Huganir RL (2000) Regulation of distinct AMPA receptor phosphorylation sites during bidirectional synaptic plasticity. *Nature* 405(6789):955–959.
5. Kristensen AS, et al. (2011) Mechanism of Ca2+/calmodulin-dependent kinase II regulation of AMPA receptor gating. *Nat Neurosci* 14(6):727–735.
6. Makino Y, Johnson RC, Yu Y, Takamiya K, Huganir RL (2011) Enhanced synaptic plasticity in mice with phosphomimetic mutation of the GluA1 AMPA receptor. *Proc Natl Acad Sci USA* 108(20):8450–8455.
7. Bredt DS, Snyder SH (1989) Nitric oxide mediates glutamate-linked enhancement of cGMP levels in the cerebellum. *Proc Natl Acad Sci USA* 86(22):9030–9033.
8. Garthwaite J (2008) Concepts of neural nitric oxide-mediated transmission. *Eur J Neurosci* 27(11):2783–2802.
9. Hess DT, Matsumoto A, Kim SO, Marshall HE, Stamler JS (2005) Protein S-nitrosylation: Purview and parameters. *Nat Rev Mol Cell Biol* 6(2):150–166.
10. Jaffrey SR, Erdjument-Bromage H, Ferris CD, Tempst P, Snyder SH (2001) Protein S-nitrosylation: A physiological signal for neuronal nitric oxide. *Nat Cell Biol* 3(2):193–197.
11. Huang Y, et al. (2005) S-nitrosylation of N-ethylmaleimide sensitive factor mediates surface expression of AMPA receptors. *Neuron* 46(4):533–540.
12. Nicoll RA, Tomita S, Bredt DS (2006) Auxiliary subunits assist AMPA-type glutamate receptors. *Science* 311(5765):1253–1256.
13. Selvakumar B, Huganir RL, Snyder SH (2009) S-nitrosylation of stargazin regulates surface expression of AMPA-glutamate neurotransmitter receptors. *Proc Natl Acad Sci USA* 106(38):16440–16445.
14. Man HY, et al. (2000) Regulation of AMPA receptor-mediated synaptic transmission by clathrin-dependent receptor internalization. *Neuron* 25(3):649–662.
15. Wang G, Moniri NH, Ozawa K, Stamler JS, Daaka Y (2006) Nitric oxide regulates endocytosis by S-nitrosylation of dynamin. *Proc Natl Acad Sci USA* 103(5):1295–1300.
16. Roche KW, O'Brien RJ, Mammen AL, Bernhardt J, Huganir RL (1996) Characterization of multiple phosphorylation sites on the AMPA receptor GluR1 subunit. *Neuron* 16(6):1179–1188.
17. Mammen AL, Kameyama K, Roche KW, Huganir RL (1997) Phosphorylation of the alpha-amino-3-hydroxy-5-methylisoxazole4-propionic acid receptor GluR1 subunit by calcium/calmodulin-dependent kinase II. *J Biol Chem* 272(51):32528–32533.
18. Lu W, et al. (2001) Activation of synaptic NMDA receptors induces membrane insertion of new AMPA receptors and LTP in cultured hippocampal neurons. *Neuron* 29(1):243–254.
19. Gopalakrishna R, Chen ZH, Gundimeda U (1993) Nitric oxide and nitric oxide-generating agents induce a reversible inactivation of protein kinase C activity and phorbol ester binding. *J Biol Chem* 268(36):27180–27185.
20. Kahlos K, Zhang J, Block ER, Patel JM (2003) Thioredoxin restores nitric oxide-induced inhibition of protein kinase C activity in lung endothelial cells. *Mol Cell Biochem* 254(1-2):47–54.
21. Song T, et al. (2008) Nitric oxide-mediated modulation of calcium/calmodulin-dependent protein kinase II. *Biochem J* 412(2):223–231.
22. Serulle Y, et al. (2007) A GluR1-cGKII interaction regulates AMPA receptor trafficking. *Neuron* 56(4):670–688.
23. Poncer JC, Esteban JA, Malinow R (2002) Multiple mechanisms for the potentiation of AMPA receptor-mediated transmission by alpha-Ca2+/calmodulin-dependent protein kinase II. *J Neurosci* 22(11):4406–4411.
24. Tomita S, et al. (2003) Functional studies and distribution define a family of transmembrane AMPA receptor regulatory proteins. *J Cell Biol* 161(4):805–816.
25. Ho GP, et al. (2011) S-nitrosylation and S-palmitoylation reciprocally regulate synaptic targeting of PSD-95. *Neuron* 71(1):131–141.
26. Tigaret CM, et al. (2006) Subunit dependencies of N-methyl-D-aspartate (NMDA) receptor-induced alpha-amino-3-hydroxy-5-methyl-4-isoxazolepropionic acid (AMPA) receptor internalization. *Mol Pharmacol* 69(4):1251–1259.
27. Erwin PA, Lin AJ, Golan DE, Michel T (2005) Receptor-regulated dynamic S-nitrosylation of endothelial nitric-oxide synthase in vascular endothelial cells. *J Biol Chem* 280(20):19888–19894.
28. Jin R, Banke TG, Mayer ML, Traynelis SF, Gouaux E (2003) Structural basis for partial agonist action at ionotropic glutamate receptors. *Nat Neurosci* 6(8):803–810.
29. Traynelis SF, Jaramillo F (1998) Getting the most out of noise in the central nervous system. *Trends Neurosci* 21(4):137–145.